



# Characterization of Surface Accumulation and Release of Nanosilica During Irradiation of Polymer Nanocomposites by Ultraviolet Light

T. Nguyen\*, B. Pellegrin, C. Bernard, S. Rabb, P. Stutzman, J. M. Gorham, X. Gu, L. L. Yu, and J. W. Chin

*National Institute of Standards and Technology, Gaithersburg, MD 20899*

Polymer nanocomposites are increasingly used in applications that are subjected to harsh environments. Owing to polymer's susceptibility to photodegradation, nanofillers in a polymer nanocomposite may be released into the environments during the composite's life cycle. Such release potentially poses an environmental health and safety problem and may hinder commercialization of these advanced materials. This study investigated the fate and release of nanosilica from epoxy/nanosilica composites. Specially-designed holders containing nanocomposite specimens were irradiated with UV light in a well-controlled environmental chamber. UV irradiated samples were removed for measurements of polymer chemical degradation, mass loss, surface morphology, nanosilica accumulation on the composite surface, and nanosilica release. Epoxy matrix underwent rapid photodegradation, resulting in substantial accumulation of silica nanofillers on the composite surface and also release from the composite. A conceptual model for surface accumulation and release of nanosilica during UV irradiation of epoxy nanocomposites is presented.

**Keywords:** Nanocomposite, SiO<sub>2</sub> Nanoparticles, Release, Accumulation, Polymer, Surface, UV, Characterization.

## 1. INTRODUCTION

Polymer nanocomposites refer to multicomponent systems in which the major constituent is a polymer or its blends and the minor constituent is a filler having at least one dimension below 100 nm (e.g., spherical nanoparticles, layered platelets, tubes, and rods). Experimental observations of large property enhancements achieved through a small addition (< 5 mass%) of nanofillers to polymers have fueled intensive research over the past decade. This is strongly evidenced in recent reviews on polymer nanocomposites for a variety of nanofillers.<sup>1–10</sup> These advanced composites are increasingly used in consumer products and in many large-volume industries such as textiles, construction, automotive, and aerospace. Under severe environmental exposure conditions, however, nanofillers may be released from the polymer nanocomposites. Because nanofillers have shown potential environmental, health and safety (EHS) risks,<sup>11–20</sup> the release of nanofillers and their EHS risks during the life cycle of a polymer

nanocomposite may present a roadblock to innovation and commercialization of these advanced materials.

There are various possible mechanisms by which nanofillers could be released during their life cycle (i.e., use, disposal, recycling, and incineration), including mechanical (e.g., abrasion, scratching, sanding, sawing), washing, matrix degradation, and fire. As such, it can be safely said that some fraction of nanofillers that have been incorporated in the polymer matrix will be released into the environment during a product's life cycles. In a recent review of nanomaterials and their effects on environmental health and safety in the construction industry, Lee et al.<sup>21</sup> have presented various possible release scenarios of nanofillers from nano-enabled products used in this industry. Gottschalk and Nowack<sup>22</sup> also briefly reviewed the release of nanofillers from products used in various applications including textiles, sunscreens, and polymer nanocomposites. Release by mechanical mechanism has been investigated for polymers containing ZnO, Fe<sub>2</sub>O<sub>3</sub>,<sup>23,24</sup> TiO<sub>2</sub>,<sup>25</sup> multi-walled carbon nanotubes (MWCNTs),<sup>26,27</sup> and SiO<sub>2</sub><sup>27</sup> nanoparticles. These studies have shown that the particles released from polymer nanocomposites by mechanical actions remain imbedded

\* Author to whom correspondence should be addressed.

in the matrix and that the size and size distribution are strongly dependent on the matrix. The emission of particles by fire of fire-retardant polymer nanocomposites containing carbon nanofibers and CNTs has been summarized in a recent review on the fate and release of CNTs.<sup>28</sup> An important finding of this summary is that no carbon nanomaterials were detected in the flame but a substantial amount of them are observed in the residual chars. Release by washing has been demonstrated in numerous reports for silver nanoparticles in polymer composites and textiles.<sup>29–32</sup>

Several studies have reported on the release of nanofillers during matrix degradation. For example, CNTs were observed suspended in solution during exposure of biodegradable polymer/CNT composites to body fluids.<sup>33,34</sup> Although no information on the chemical composition of the released particles was given, it is likely that the released materials were individual or aggregates of CNTs that are free of the matrix. The effect of ultraviolet (UV) radiation was included in a recent investigation on nanoparticle release and the *in-vivo* risks this may pose for polymer and cement nanocomposites.<sup>27</sup> This study reported that photodegradation of a photo-labile thermoplastic has resulted in a slow release of MWCNTs from polymer nanocomposite, but no nanosilica was observed to be released from a polyamide/nanosilica composite, exposed to UV radiation. The release of nanosize particles from a paint containing anatase TiO<sub>2</sub> nanofillers exposed to a simulated environment of UV radiation, wind, and human contact has been observed.<sup>35</sup> A similar result has been reported for polymer and wood surfaces containing the same nanofiller. This study noted that the amount of released TiO<sub>2</sub> nanomaterials was much less in the absence of UV radiation. The release of this nanofiller from polymer nanocomposites is not surprising, because anatase TiO<sub>2</sub> is known to be photoreactive material.<sup>36</sup> In the presence of UV radiation, it accelerates the degradation of polymer thereby exposing TiO<sub>2</sub> particles at the surface (i.e., chalking phenomenon). An analysis of runoff water from new and aged facade paints showed the presence of nano TiO<sub>2</sub> and suggested that the nanofillers were detached from these surfaces by natural weathering.<sup>37</sup> The released TiO<sub>2</sub> nanofillers were reported to partially embed in the polymer matrix.

Most common polymers used in high-volume industries tend to undergo some form of degradation when they are exposed to UV, moisture, temperature, ozone, acid rains, or combinations thereof.<sup>38</sup> When the matrix is chemically degraded and removed from the nanocomposite, the nanofillers that are left on the product surface or released into the environment are likely not coated with the polymer material. This has been demonstrated for paints containing nanoTiO<sub>2</sub> degraded by natural weathering.<sup>37</sup> Such bare nanofillers have been shown to cause adverse effect on human health and the environment, as indicated earlier.

Furthermore, because the bonding between a typical polymer and an inorganic particle is governed by weak secondary forces and easily broken in the presence of water or high humidity,<sup>39</sup> any chemically-degraded polymer film that still adheres to the nanoparticle surface can be y detached during exposures. Matrix degradation will also cause extensive oxidation, chain scission, and crosslinking of the polymer chains, which increases brittleness, loss of mechanical properties, and cracking of the polymer nanocomposites. This will increase the possibility of nanofiller migration and release. Mechanical vibrations, rain, condensed water, snow, and wind will likely increase the release rate. Once released, nanofillers may undergo physical and chemical transformations, which may change their properties and risk impacts.

The degradation of the matrix in a polymer nanocomposite is inherently a complex function of the environmental conditions and the material properties. However, the outdoor weathering factors are neither controllable nor repeatable. Therefore, an accurate prediction of nanofiller release rate for polymer nanocomposites during their use in an outdoor environment is difficult. On the material side, the presence of a large, undefined polymer/particle interfacial volume fraction in the nanocomposites and the unique electronic structure of the incorporated nanofillers will likely affect the degradation rates and mechanisms of both the polymer matrix and the nanofiller release. For example, a study by Gu et al.<sup>40</sup> with ZnO nanofillers has shown that, instead of stabilizing the photodegradation as reported previously,<sup>41,42</sup> this nanofiller actually accelerated the degradation of a polyurethane matrix under UV radiation.

Despite the serious potential risks posed by nanofiller release during the life cycle of polymer nanocomposites, little data is available about the degradation mechanism of these advanced materials, the fate of embedded nanofillers during environmental exposures of nanocomposites, or how they may be released during the product's life cycle. This lack of information hinders our ability to understand the release mechanism, to predict the release rate, and to develop strategies for mitigating this potentially serious problem. Therefore, the long term performance and the potentially harmful effects of the nanofillers incorporated in polymer matrices on the EHS cannot be determined. To provide data needed to address these issues, researchers from the National Institute of Standards and Technology have initiated a series of studies to critically assess the release of nanofillers during life cycles of polymer nanocomposites. The study consists of four main tasks:

- (1) Develop methods to characterize the degradation of polymer nanocomposites, nanofiller release rates, and chemical composition of released particles during life cycle of nanocomposites,
- (2) generate microscopic and molecular experimental data to provide a scientific-based understanding of the nanofiller release mechanism,

- (3) develop experimentally-verified models to predict the nanofiller release that takes into account materials and environmental factors as inputs, and
- (4) develop standards for measurements of the release rate and properties of the released nanofillers.

This research is in line with the current United States National Nanotechnology Initiative EHS Research Strategy for nanotechnology, which focuses on the risks and hazards during life cycle of the nano-enabled products.<sup>43</sup>

Previously, we have reported the accumulation of a thick layer of MWCNT or graphene oxide on nanocomposites surface during their exposure to UV radiation.<sup>44–46</sup> For MWCNTs, we found little evidence of their release into the environment even after prolonged exposure. (No such statement can be made for polymer/graphene oxide nanocomposite, because no extended UV exposure study was conducted for this nanoparticle). The present study investigates the fate and release of spherical SiO<sub>2</sub> nanofillers (nanosilica) in an amine-cured epoxy matrix irradiated with UV light in the 295 nm to 400 nm range. An UV environment was selected because it is the most detrimental component among weathering factors. On the other hand, amine-cured epoxy is used extensively in fiber-reinforced polymer composites, protective coatings, and structural adhesives for exterior applications. SiO<sub>2</sub> nanofillers are increasingly used in these materials,<sup>9,47–51</sup> and their adverse effects on the environment and health have been documented.<sup>52–56</sup>

Composite films of epoxy matrix containing 5% and 10% SiO<sub>2</sub> nanofillers were fabricated, irradiated with UV radiation in a well-controlled environmental chamber, and characterized for fate and release of SiO<sub>2</sub>. Characterization was performed by a number of microscopic and spectroscopic techniques, including scanning electron microscopy (SEM), atomic force microscopy (AFM), Fourier transform infrared spectroscopy (FTIR), inductively coupled plasma-optical emission spectrometry (ICP-OES), and X-ray photoelectron spectroscopy (XPS). In addition, a special sample holder was fabricated for simultaneous UV irradiation of nanocomposite samples and collection of the released nanofillers. The results showed that, under UV radiation having wavelengths approximating those of sunlight, the amine-cured epoxy matrix underwent rapid photodegradation, resulting in substantial mass loss, a significant accumulation of SiO<sub>2</sub> nanofillers on the irradiated nanocomposite surface, and release of nanoparticles from the composite. A conceptual model is presented to describe the accumulation and release process. The results of this study should provide useful information to assess the potential risk of spherical nanofillers in epoxy matrix during its service in an UV environment.

## 2. EXPERIMENTAL DETAILS

### 2.1. Materials and Nanocomposite Preparation

Nanosilica (SiO<sub>2</sub> nanofillers) (Aerosil R812, Evonik) is a hydrophobic material, having an average primary diameter of 7 nm and a purity > 99.8%. The surface of this SiO<sub>2</sub> material was modified with hexamethyl disilazane, where most of the surface SiOH (silanols) are protected by trimethylsilyl groups (Si–O–Si(CH<sub>3</sub>)<sub>3</sub>) with only 0.29 free OH groups/nm<sup>2</sup>.<sup>57</sup> The nanofillers form aggregates and agglomerates with a very large specific surface area (typically 260 ± 30 m<sup>2</sup>/g). The epoxy matrix was a model stoichiometric mixture of a diglycidyl ether of bisphenol A (DGEBA) epoxy resin (EPON 828, Resolution Performance Products) having an equivalent mass of 189 (grams of resin containing one gram equivalent of epoxide) and a tri-polyetheramine curing agent (Jeffamine T403, Huntsman Corporation). There were no additives added to the amine-cured epoxy matrix. The chemical structures of the components and cured epoxy are illustrated in Figure 1. It should be noted that, due to steric hindrance and restricted transport during the late curing stages, unreacted epoxide and amino groups are expected to be present in the matrix after curing. The presence of these functional groups and impurities (e.g., residual catalyst, oxidation stabilizers) may have an influence on the photodegradation of an amine-cured epoxy. The solvent used for nanocomposite processing was reagent grade toluene (purity > 99.5%) (Aldrich).

Free-standing nanocomposite films having a thickness range between 200 μm and 250 μm of the amine-cured epoxy polymer containing 5% and 10% mass fractions of SiO<sub>2</sub> nanofillers were prepared following the steps illustrated in Figure 2. SiO<sub>2</sub> nanofillers were first sonicated in a large amount of toluene for 30 minutes using an 80 kHz tip sonicator. After adding the appropriate amount

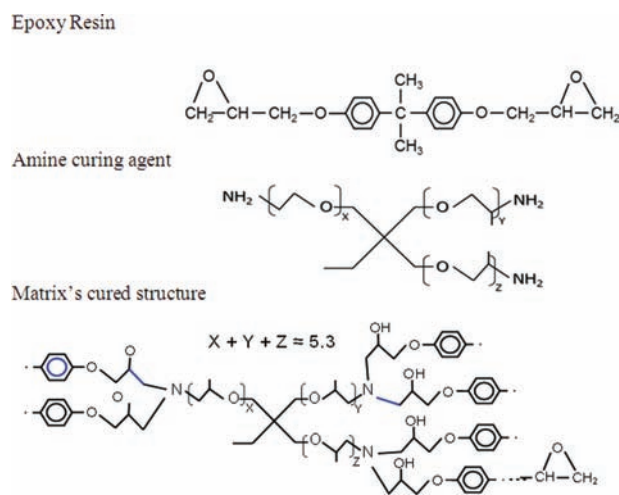
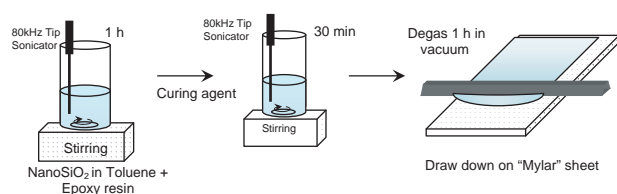


Fig. 1. Chemical structures of the components and cured epoxy matrix used in this study.



**Fig. 2.** Steps used to prepare epoxy/nanosilica composite films.

of epoxy resin, the nanofiller suspension was sonicated under constant stirring with a magnetic stirrer for an additional 1 hour. The amine curing agent was then added to the suspension, and the mixture was sonicated for another hour. Unfilled (neat) epoxy films having similar thickness were also prepared for comparison by mixing appropriate amounts of amine curing agent and epoxy resin. The mixture was stirred for 1 hour with a mechanical stirrer. After the mixing step, both the nanosilica-free and epoxy/nanosilica mixtures were degassed for 1 hour at room temperature and then drawn down on a polyethylene terephthalate sheet (Mylar) (a good release substrate for epoxy-base materials). Films were cured at ambient conditions (24 °C and 50% relative humidity) for three days, followed by post-curing for 4 hours at 110 °C in an air circulating oven.

## 2.2. UV Irradiation Condition

All UV irradiation experiments were carried out using the NIST 2 m integrating sphere-based UV chamber, referred to as SPHERE (Simulated Photodegradation via High Energy Radiant Exposure) described in detail previously.<sup>58</sup> This SPHERE UV chamber utilizes a mercury arc lamp system that produces a collimated and highly uniform UV flux of approximately 480 W/m<sup>2</sup> in the 290 nm to 450 nm range. The visible and infrared radiation of the SPHERE's UV source has been removed; therefore, without external heating, the temperature in this UV chamber is about

27 °C ± 2 °C. This UV chamber can also precisely control the relative humidity (RH) and temperature.

Except for studying nanofiller release where larger sample sizes were used, specimens for other measurements of neat matrix and nanocomposites having dimensions of 25 mm × 25 mm were first mounted in a 17-window sample holder (Fig. 3(a)), which was irradiated in the SPHERE UV chamber at 50 °C and 70% RH. Note that because the window diameter of the sample holder used in this study was 19 mm, only the surface area within this diameter was irradiated. Specimens were removed after specified accumulated doses (i.e., at specified time intervals) for characterization. Dose, in kJ/m<sup>2</sup>, is defined here as the total accumulated energy resulting from repeated UV radiation exposures at a particular time period per unit irradiated surface. For the nanofiller release study, a specially-designed sample holder (Figs. 3(b and c)) was employed. This holder collected particles released during UV irradiation of the polymer nanocomposites. It consisted of a sample chamber, tubes to supply desired RH and temperature, and a container to collect released particles. A cover containing a quartz window that allows UV to irradiate the sample was used to seal the holder. In this study, a poly(tetrafluoroethylene) film was placed on the collector surface. All specimens were mounted so that their faces were perpendicular to the horizontal plane.

## 2.3. Characterization of UV-Irradiated Samples

Mass loss, surface morphology, chemical degradation, and amounts of SiO<sub>2</sub> nanofillers accumulated on sample surface and released to the environment as a function of UV irradiation were characterized or measured. The mass loss was determined using an analytical balance having a resolution of 10<sup>-5</sup> g. Surface morphological changes were followed by atomic force microscopy (AFM) and field emission scanning electron microscopy (FE-SEM). FE-SEM (HITACHI S-4700) imaging was operated at 1 KeV.

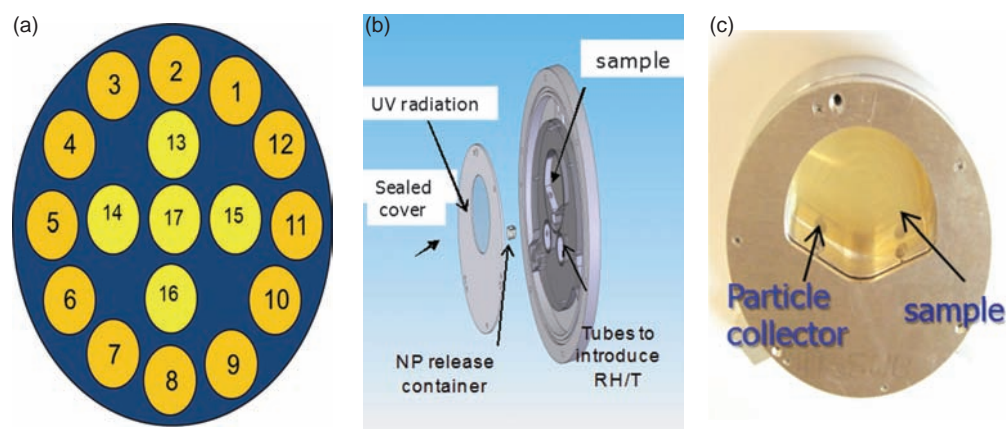


**Fig. 3.** (a) 17-window sample holder for UV irradiation of polymer nanocomposites, (b) schematic of the sample holder to collect released nanofillers, and (c) photograph of the nanofiller release holder containing an UV irradiated epoxy/nanosilica composite sample.

AFM measurements were carried out at ambient conditions (24 °C, 50% relative humidity) using a Dimension 3100 system (Veeco Metrology) and silicon probes (TESP 70, Veeco Metrology). Both topographic (height) and phase images were obtained simultaneously using a resonance frequency of approximately 300 kHz for the probe oscillation and a free-oscillation amplitude of  $62 \text{ nm} \pm 2 \text{ nm}$ .

The chemical degradation of neat matrix and nanocomposites was measured using Fourier transform infrared spectroscopy in the attenuated total reflection (FTIR-ATR) mode and X-ray photoelectron spectroscopy (XPS). FTIR spectra were recorded at a resolution of  $4 \text{ cm}^{-1}$  using dry air as a purge gas and a spectrometer (Nexus 670, Thermo Nicolet) equipped with a liquid nitrogen-cooled mercury cadmium telluride (MCT) detector. A ZnSe prism and a  $45^\circ$  incident angle were used for the FTIR-ATR measurement. All spectra were the average of 128 scans. The peak height was used to represent the infrared intensity, which is expressed in absorbance, A. All FTIR results were the average of four specimens. XPS analyses were carried out using a 5400 spectrophotometer (Physical Electronics) equipped with a non-monochromated Mg  $K\alpha$  X-ray source (1253.6 eV) at a  $45^\circ$  angle between the sample surface normal. Spectra were acquired at a pass energy 44.75 eV and a step size of 0.125 eV/step for the C(1s), Si(2p), O(1s) and N(1s) regions. All XPS spectra were fit with a Shirley baseline, and adjusted with the appropriate sensitivity factors to obtain information on percent composition. The released particles were imaged by FE-SEM at 7 KeV and their chemical information was studied by Energy Dispersive X-ray Spectroscopy (EDS) in the SEM. It is noted that XPS, SEM, and AFM characterizations were performed only on 5% nanosilica composite samples.

The amounts of  $\text{SiO}_2$  nanofillers accumulated on nanocomposite surface as a function of UV irradiation were measured by ICP-OES. Briefly,  $25 \text{ mm} \times 25 \text{ mm}$  specimens of neat epoxy and 5% and 10% nanosilica composite films after 59 day irradiation were extracted using a 5% hydrofluoric acid (HF) solution for 5 min. After removing the films, the extracted solutions were diluted and neutralized with 0.2% NaOH solution before analyzing by ICP-OES (PerkinElmer Optima 5300DV). Un-irradiated specimens of the same neat and nanosilica composite films were extracted similarly to serve as blank references. Each extracted solution was then split into two equal parts, and one part was spiked with a known amount of Si. The concentrations of Si-spiked solutions ranged from  $0.38 \mu\text{g/g}$  Si to  $2.7 \mu\text{g/g}$  Si and were prepared using the standard reference material (SRM) 3150 Silicon Standard Solution. Sn was used as an internal standard. More complete details of this measurement have been given elsewhere.<sup>59</sup>

### 3. RESULTS

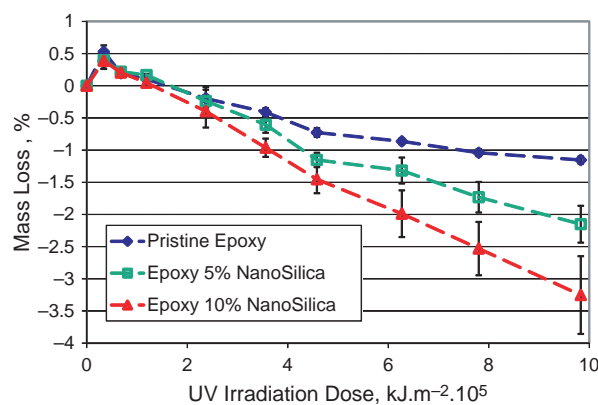
#### 3.1. Mass Loss of Epoxy/Nanosilica Composite with UV Irradiation

Figure 4 displays the total mass loss of neat epoxy and epoxy/nanosilica composite specimens as a function of accumulated UV irradiation dose at 50 °C and 70% RH. The mass loss is expressed as  $[(\text{initial mass} - \text{mass at any irradiation dose}) / \text{initial mass}] \times 100$ . Except for a small increase at early exposures, the mass loss in both materials was nearly linear with irradiation dose. The early increase was due probably to the water uptake in the material, which was greater than the degradation-induced material loss. This is because these specimens were exposed to 70% RH and, thus, the amount of sorbed water in the specimen was substantial. Figure 4 shows that both the rate and amounts of mass loss of the nanocomposites were higher than those for neat epoxy, and that these quantities were greater with higher nanosilica loading. The average mass losses for neat epoxy, epoxy/5% nanosilica composite, and epoxy/10% nanosilica composite irradiated with  $9.8 \times 10^5 \text{ kJ/m}^2$  UV dose were 1.2%, 2.2%, and 3.3% respectively.

Figure 4 Mass loss as a function of irradiation dose for neat epoxy and epoxy/nanosilica composites irradiated with UV radiation at 50 °C/70% RH condition. Each data point was the average of six specimens, and error bars represent one standard deviation.

#### 3.2. Chemical Degradation of Epoxy/Nanosilica Composites with UV Irradiation

Amine-cured epoxy polymers are used extensively in many exterior applications. However, due to the presence of electron-rich nitrogen atom and UV-absorbing aromatic ring in the chemical structure, photodegradation of epoxy-based products has been extensively studied using



**Fig. 4.** Mass loss as a function of irradiation dose for neat epoxy and epoxy/nanosilica composites irradiated with UV radiation at 50 °C/70 % RH condition. Each data point was the average of six specimens, and error bars represent one standard deviation.

both short monochromatic and long polychromatic long wavelength (60–66). Under short UV radiation (254 nm), bisphenol A epoxy molecule in an epoxy network undergoes direct chain scission and side group abstraction to form free radicals, which then go through free radical mechanisms to form various oxidation products and loss of materials. For UV radiation wavelength >295 nm, which is present in the sun's spectrum at ground level, degradation is believed to be through a photo-oxidation process, in which the free radicals generated by chromophoric impurities initiate the photodegradation by abstraction of hydrogen from the polymer chains. In either short or long wavelength cases, chain scission is accompanied by crosslinking. The photochemical degradation processes lead to loss of performance of the epoxy composites, such as decrease in mechanical property, yellowing, and cracking.

The FTIR-ATR technique was used to follow the chemical degradation of the matrix in the epoxy/nanosilica composites as a function of UV irradiation. The probing depth of the ATR technique is a function of incident angle, IR wavelength, and refractive indices of both the internal reflection element (i.e., prism) and the polymer. For the ZnSe prism and 45° incident angle used in this study, the probing depth in the epoxy polymer (refractive index 1.5) in the region between 800  $\text{cm}^{-1}$  and 3600  $\text{cm}^{-1}$  (12.5  $\mu\text{m}$  and 2.7  $\mu\text{m}$ ) is between 0.5  $\mu\text{m}$  and 2.5  $\mu\text{m}$  from the surface. The probing depth in a silica material (refractive index 1.46) is slightly greater than that in the polymer. Therefore, any chemical changes in the epoxy/nanosilica composites resulted from the UV irradiation reported here originated from the material layer at or near the exposed composite surface.

Although FTIR-ATR spectra recorded at different irradiation doses can provide useful information (not shown) about the chemical changes of the polymer nanocomposites, chemical degradation of polymers is better studied using the FTIR difference spectroscopy method, in which gain or loss of a particular functional group can be easily discerned. Figure 5 shows difference FTIR-ATR spectra of the epoxy/5% nanosilica composite for different irradiation doses. These spectra were obtained by subtracting the spectrum of the un-irradiated (unexposed) specimen from that recorded at different irradiation doses on the same specimen after normalizing to a reference band to account for any effect due to sampling. In a difference spectrum, bands below and above the zero absorbance line represent a loss (e.g., chain scission) and a gain (e.g., oxidation), respectively, of a functional group in the sample. Figure 5 shows that the intensities of numerous bands of the epoxy structure substantially decreased, including the bands at 1508  $\text{cm}^{-1}$  due to benzene ring, 1245  $\text{cm}^{-1}$  due to aromatic ether, and new bands in the 1620  $\text{cm}^{-1}$ –1740  $\text{cm}^{-1}$  region, due to the formation of C=C and various carbonyl groups (C=O), such as aldehydes, ketones, and amides

have appeared, similar to those reported previously for amine-cured epoxy (61–66). These changes are attributed to photo-oxidation of the chemical structure by 295 nm to 400 nm UV radiation, leading to extensive chain scission of the main chains of the epoxy. Details regarding photodegradation mechanism of amine-cured epoxies are beyond the scope of the present study but may be found in Refs.[60]–[65]). Carbonyl groups formed can absorb radiation at long wavelengths and accelerate the degradation. UV-visible transmission spectra (not shown) exhibited a progressive increase of the absorbance intensity in the region above 300 nm, indicating that the degraded epoxy films did absorb UV light at longer wavelengths. Both the neat epoxy and epoxy/nanosilica composite films also showed increasing yellowing with UV irradiation, suggesting that a substantial amount of conjugated structures had formed in this epoxy matrix. Our previous extensive study has demonstrated that UV radiation is the major weathering factor that causes severe degradation of amine-cured epoxies, with temperature and RH playing a minor role.<sup>67</sup>

The bands at 1245  $\text{cm}^{-1}$  and 1714  $\text{cm}^{-1}$ , representing chain scission and oxidation of the epoxy, respectively, and at 1180  $\text{cm}^{-1}$ , attributed to contributions of C–O and Si–O bonds, were used to follow various degradation processes of the epoxy matrix and the accumulation of SiO<sub>2</sub> at or near the nanocomposite surface during UV irradiation. Intensity changes of these bands with irradiation dose are displayed in Figure 6. The intensity values have been normalized to both the initial absorbance and that of the least-changed band (1360  $\text{cm}^{-1}$ , due to CH<sub>3</sub> of gem-dimethyl) to minimize the sampling effect by the ATR technique. This normalization is essential for polymer degradation study by the FTIR-ATR technique because, as the degradation becomes more severe, the surface becomes rougher and stiffer, which affects the band intensity. Information about the behavior of the 1360  $\text{cm}^{-1}$  band with UV irradiation was obtained from a parallel quantitative transmission FTIR study of a thin (7  $\mu\text{m}$ ) spin casting film on

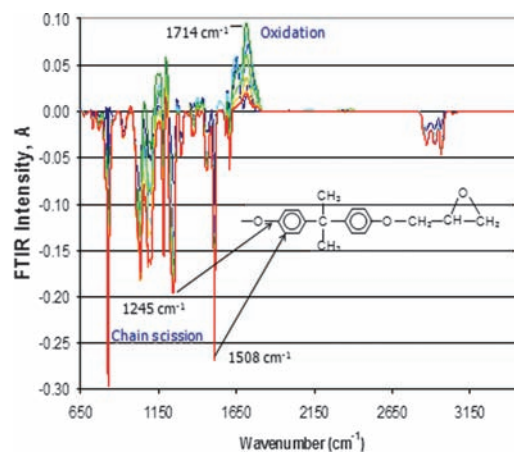


**Fig. 5.** Difference FTIR-ATR spectra of epoxy/5% nanosilica composite recorded at different UV irradiation doses.

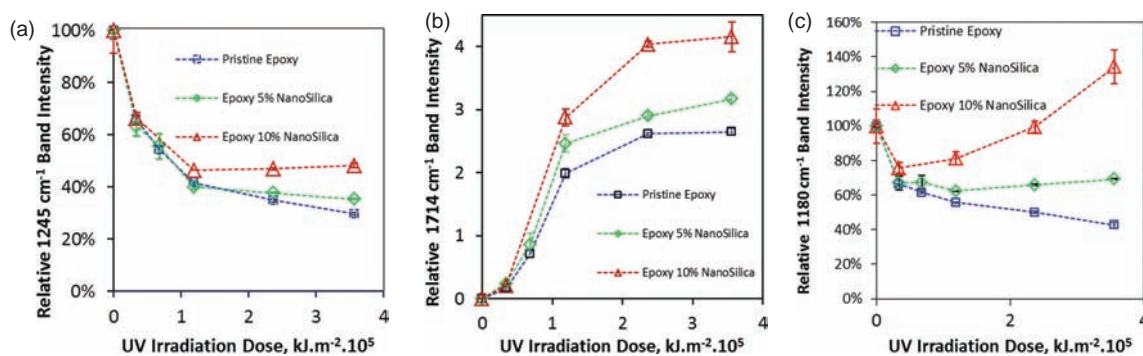


**Fig. 6.** FTIR-ATR intensity changes with irradiation dose for: (a) 1245  $\text{cm}^{-1}$ , (b) 1714  $\text{cm}^{-1}$ , and (c) 1180  $\text{cm}^{-1}$  bands for neat (pristine) epoxy and nanocomposites before and after irradiated with UV radiation. Each data point was the average of four specimens, and the error bars represent one standard deviation.

a  $\text{CaF}_2$  substrate. The intensity of this 1360  $\text{cm}^{-1}$  band (not shown) of the transmission spectrum showed little change for the irradiation dose of  $3.5 \times 10^5 \text{ kJ/m}^2$  or lower under the same irradiation condition. Thus, all quantitative FTIR-ATR analyses were up to but not exceeding this dose value. In addition, because the 1714  $\text{cm}^{-1}$  band was formed only after the UV irradiation, its initial absorbance value was arbitrarily set to 1, strictly for comparison purposes. The error bars in Figure 6 show small standard deviations between specimens, indicating good reproducibility of the data.

Figures 6(a) and (b) indicated that, under the UV irradiation conditions used, both neat epoxy and epoxy/nanosilica composite films underwent rapid photodegradation with extensive chain scission and formation of a substantial amount of oxidized products under UV exposure. The photodegradation appeared to level off after irradiation to approximately  $1.2 \times 10^5 \text{ kJ/m}^2$  dose. However, differences in the FTIR intensity exist between the neat epoxy and nanocomposite films between  $1.2 \times 10^5 \text{ kJ/m}^2$  and  $3.5 \times 10^5 \text{ kJ/m}^2$  irradiation doses. The intensity decrease due to chain scission was smaller, and intensity increase due to oxidation was greater, with increasing nanosilica loading. An examination of the intensity change of the same bands in the transmission FTIR spectra (not shown) for thin film ( $7 \mu\text{m}$ ) specimens of the same materials irradiated under the same conditions revealed essentially no difference in the chain scission or oxidation rates between the neat epoxy and the nanocomposite films. The transmission FTIR result suggested that the nanosilica material used neither catalyzed nor stabilized the photodegradation of this amine-cure epoxy.

Therefore, the intensity difference at irradiation doses greater than  $1.2 \times 10^5 \text{ kJ/m}^2$  observed in Figure 6 may be attributed partially to the  $\text{SiO}_2$  nanofiller layer on the composite surface (clearly seen in the microscopic images shown in Section 3.3), which was formed during UV irradiation. Although the exact effect of the surface nanosilica layer on the FTIR results of Figure 6 is unclear, the presence of a surface layer consisting of large surface area

particles that have a lower refractive index (than that of the matrix) will likely have a complex influence on the optical properties (transmission/reflection) of both the impinging UV radiation and the ATR-generated evanescent waves (to detect IR signal). As revealed later in the ICP results, 5% and 10% nanosilica loadings produced approximately 320 nm and 753 nm thick, respectively,  $\text{SiO}_2$  nanofiller layers on the irradiated composite surfaces. Further, the ATR probing depth is slightly greater in the silica material than in the polymer. Therefore, the higher intensity of the C=O band at 1714  $\text{cm}^{-1}$  at higher nanosilica loading seen in Figure 6(b) may be attributed to a deeper sampling of the nanosilica-covered surface and/or multiple reflections of the evanescent waves, which also increased the signal detected. For the chain scission band at 1245  $\text{cm}^{-1}$ , a band of the  $\text{SiO}_2$  nanofillers, which extends from 1000  $\text{cm}^{-1}$  to 1250  $\text{cm}^{-1}$ , probably contributed to the higher intensity at irradiation dose greater than  $1.2 \times 10^5 \text{ kJ/m}^2$  observed in Figure 6(a).

This postulation is in agreement with the result of Figure 6(c), which displays intensity changes of the 1180  $\text{cm}^{-1}$  band with irradiation dose. The intensity of this band for the 10% nanosilica composite material decreased at very low dose but rose sharply at irradiation doses greater than  $1.7 \times 10^5 \text{ kJ/m}^2$ , suggesting that the concentration of  $\text{SiO}_2$  nanofillers on the surface had increased. The decrease at low dose is attributed to the intensity loss of the epoxy C–O band. At higher doses, the intensity of this band also decreased, but at a lower rate than that due to the increase of the Si–O band. The 5% nanosilica composite showed a similar trend but at a lesser extent. The FTIR results shown in Figure 6(c) for 5% nanosilica composite are consistent with SEM and AFM observations shown in Section 3.3.

The degradation of the epoxy matrix and an increase of the  $\text{SiO}_2$  material near the nanocomposite surface is consistent with the XPS results displayed in Figure 7 for 5% nanosilica composite. As the irradiation dose increased from 0  $\text{kJ/m}^2$  to  $10.07 \times 10^5 \text{ kJ/m}^2$ , the percent surface concentration of carbon decreased from  $82.2\% \pm 1.7\%$  to

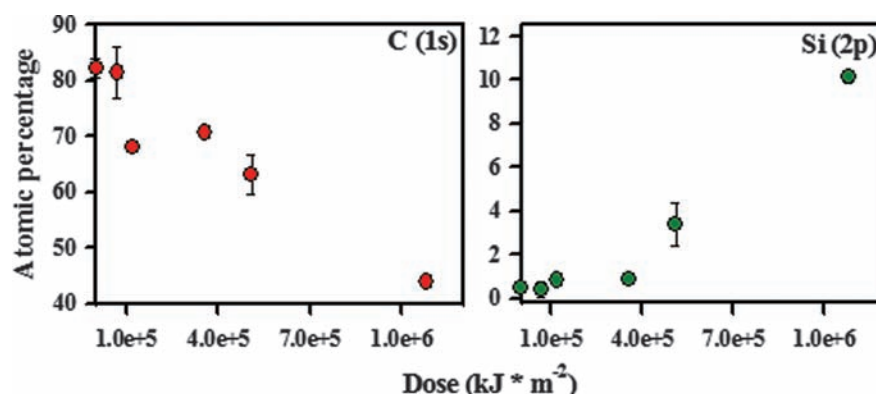


**Fig. 7.** XPS-based carbon and silicon atomic percentages on the epoxy/nanosilica composite surface versus UV irradiation dose. Except for the  $3.56 \times 10^5$  kJ/m<sup>2</sup> dose result where only one specimen was used, other data points consisted of two or more specimens with the error being representative of  $\pm$  one standard deviation.

43.8%  $\pm$  0.7%, while that of silicon increased from 0.5%  $\pm$  0.1% to 10.1%  $\pm$  0.3%; the balance of the composition was made up of nitrogen and oxygen.

Additionally, there was a period of no significant carbon loss and even greater doses were required to observe a large increase in the silicon percent concentration, consistent with the mass loss measurement in Figure 4 which showed no significant mass loss until an irradiation dose of  $\geq 3.0 \times 10^5$  kJ/m<sup>2</sup>. The increase of SiO<sub>2</sub> on the composite surface following UV irradiation has also been confirmed and quantified by ICP-OES analysis.

### 3.3. Surface Morphological Changes of Epoxy/Nanosilica Composites with UV Irradiation

Characterizing the surface morphology of polymeric materials during environmental exposures can provide a good insight on microstructure, chemical homogeneity, and degradation activity (e.g., autocatalytic) occurring on a polymeric material surface.<sup>68–70</sup> This information is helpful for understanding the degradation mechanism and degradation mode (i.e., localized or uniform degradation) of polymer systems. For polymer nanocomposites, imaging at the nanoscale spatial resolution of a sample surface during environmental exposures would, in addition to matrix degradation behavior, provide important data to assess the fate of nanofillers. This has been demonstrated for nanocomposites exposed to hydrolytic and photolytic environments. For example, SEM analysis by Armentano et al.<sup>71</sup> has shown that the hydrolysis of poly(DL-Lactide-co-glycolide) (PLGA) containing pristine single-walled carbon nanotubes (SWCNTs) in biological fluid is a localized process, giving rise to large pores and CNT bundles on the composite surface without evidence of CNT release to the environment. However, for the same matrix containing SWCNTs-COOH nanofillers, the degradation is accelerated and the degraded surface appears uniform. This degradation resulted in a release of SWCNTs-COOH

to the biological medium, which can be observed with UV-visible spectroscopy and color change of the solution. Similarly, using AFM, Gu et al.<sup>40</sup> observed the formation of large, deep pits in polyurethane/nanoZnO composites irradiated with UV light. Nanofillers were found on the pit bottom surface, suggesting that the pit formation was initiated and accelerated locally by the photo-catalyzed ZnO nanofillers. On further exposure and/or in the presence of rain or condensed water, the surface-exposed nanofillers may be released to the environments.

In this study, morphological changes of epoxy/nanosilica composite surfaces as a function of UV irradiation dose were studied by FE-SEM and tapping mode AFM. Figure 8 displays FE-SEM backscattering images at two different magnifications of epoxy/5% nanosilica composite for varying irradiation doses. The un-irradiated nanocomposite surface appeared smooth with evidence of some SiO<sub>2</sub> nanofillers (Fig. 8, far left, lower row). After UV irradiating with a  $0.67 \times 10^5$  kJ/m<sup>2</sup> dose, a substantial amount of SiO<sub>2</sub> nanofillers has appeared on the surface. With further irradiation, the surface concentration of nanosilica continued to increase, and after  $7.0 \times 10^5$  kJ/m<sup>2</sup> dose, a layer of compact SiO<sub>2</sub> nanofillers has covered almost the entire composite surface. Figure 8 also revealed other features that are of interest. For example, it showed that the SiO<sub>2</sub> nanofillers appeared to aggregate and form a layer on the surface. The lower magnification SEM image at  $7.0 \times 10^5$  kJ/m<sup>2</sup> dose revealed a crack in the nanosilica-rich surface layer (upper right, arrowed), which may affect the nanosilica release. It is not known whether the crack was formed during the UV irradiation or induced by the SEM vacuum environment. In addition, the low magnification images at  $0.67 \times 10^5$  kJ/m<sup>2</sup> and  $1.2 \times 10^5$  kJ/m<sup>2</sup> doses (top row) showed that the initial dispersion of SiO<sub>2</sub> nanofillers in the epoxy matrix was good.

Figure 9 displays height and phase AFM images at two magnifications for un-irradiated (upper row) and  $7.0 \times 10^5$  kJ/m<sup>2</sup> UV irradiated (lower row) epoxy/5% nanosilica

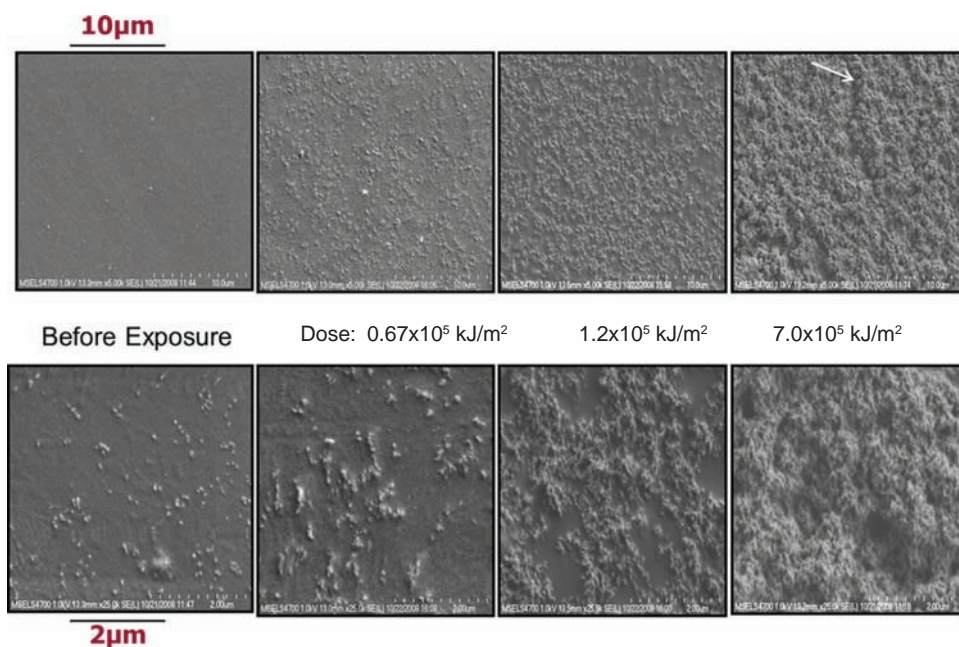


Fig. 8. FE-SEM images at two magnifications of epoxy/5% nanosilica composite surface before and after UV irradiating with different doses.

composites. Both height and phase images at low magnification (upper row, two left images) show the presence of nanofillers on the surface, similar to that observed by SEM at high magnification. However, the presence of SiO<sub>2</sub> nanofiller clusters on the un-irradiated nanocomposite surface is clearly seen by the phase image at the higher magnification (upper row, far right). The brightness of these nanofillers in the height image (upper row, second from right) indicates that they were raised above the surface. The AFM phase image at lower magnification (lower row, second from left) show clearly that the surface was nearly covered with SiO<sub>2</sub> nanofillers after irradiation with a  $7.0 \times 10^5$  kJ/m<sup>2</sup> dose, similar to that observed with SEM. Figure 9 also revealed that, although both topographic and phase imaging AFM are suitable for following the accumulation of nanosilica on the UV irradiated nanocomposite surface, the latter imaging mode provides a stronger con-

trast between the hard inorganic SiO<sub>2</sub> nanofiller and the viscoelastic epoxy matrix than that of the former. Because AFM is usually operated at ambient conditions, the results demonstrated that phase imaging AFM is a convenient technique to effectively follow the accumulation of inorganic nanofillers on polymer nanocomposite surface during UV irradiation. Although relative humidity in the 30% and 80% range has been demonstrated to strongly enhance the AFM image contrast,<sup>72</sup> the effect of 50% RH used in this study on the contrast of Figure 9 images was not measured.

#### 3.4. Quantifying the Amount of SiO<sub>2</sub> Nanoparticles Accumulated on UV Irradiated Nanocomposite Surface

Figures 8 and 9 clearly show the presence of a layer of SiO<sub>2</sub> nanofillers on the UV-irradiated surface. However, these qualitative microscopic results cannot be used for kinetic studies of nanosilica formation on nanocomposite surface with irradiation. To determine the amounts of SiO<sub>2</sub> nanofillers accumulated on the surface during UV irradiation, a chemical extraction method using HF solution was developed to selectively dissolve SiO<sub>2</sub> nanofillers on the composite surface with minimal extraction of the nanofillers from the interior of the nanocomposite. The extracted solution was then analyzed by ICP-OES. A preliminary experiment was conducted to determine the appropriate HF concentration and extraction time. Variable volume concentrations of HF in water from 1% to 50% were first tested using SiO<sub>2</sub> nanofillers alone (sample size < 10 mg). Different concentrations of HF were prepared by first adding water to the nanofillers, followed by

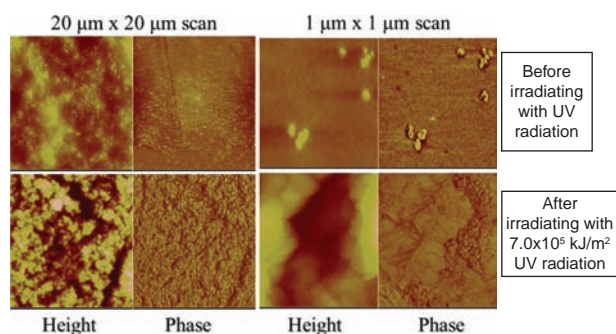
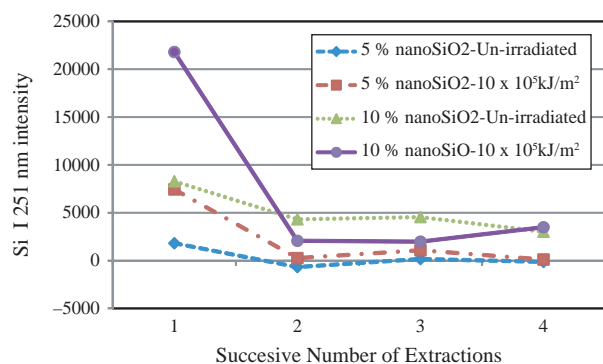


Fig. 9. AFM images at two magnifications of epoxy/5% nanosilica composite before and after irradiating with  $7.0 \times 10^5$  kJ/m<sup>2</sup> UV radiation. For each AFM pair, height image is on the left and phase image is on the right.

adding concentrated HF to the suspension to give a total of 10 mL. It was observed that volume concentrations of HF from 10% to 50% dissolved the SiO<sub>2</sub> nanofillers in 1 min or less. The dissolution rate at these HF concentrations was deemed too rapid and could potentially attack a substantial amount of SiO<sub>2</sub> nanofillers embedded in the polymer matrix. At 1% HF and 5% HF concentrations, the SiO<sub>2</sub> nanofillers were dissolved in approximately 15 min and 2 min, respectively. Of the two concentrations, 5% HF was chosen as the extraction solution because the dissolution time is not excessively long. Further, although a 2 min extraction time was found adequate for completely dissolving a 10 mg sample of SiO<sub>2</sub> nanofillers, all experiments for nanocomposites used a 5 min extraction time to ensure that all (or most) SiO<sub>2</sub> nanofillers located on the nanocomposite surface were dissolved.

To assess the effect of the extraction solution on the SiO<sub>2</sub> nanofillers in the nanocomposite interior, an experiment involving a successive number of extractions was conducted. This experiment was carried out as follows. After immersing a nanocomposite specimen in a 5% HF extraction solution for 5 minutes, the solution was analyzed for Si by ICP-OES. After removing from the extracted solution and washing thoroughly with water, the specimen was re-immersed in a fresh extraction solution for the same length of time, and the amount of Si measured. The same procedure was repeated for a 3rd and 4th time. The results are displayed in Figure 10, which shows the intensity of Si I 251 nm as a function of four successive extractions for 5% and 10% nanosilica nanocomposites before and after  $10 \times 10^5$  kJ/m<sup>2</sup> UV irradiation. This preliminary experiment used only one specimen for each type of nanocomposite film; therefore, no uncertainty is given. However, the errors by ICP-OES analysis and the reproducibility of the extraction procedure are low (uncertainty is < 10 %). Figure 10 shows little change in Si concentration in the extracted solution after the first extraction for all four types of sample, suggesting that little dissolution of the interior SiO<sub>2</sub> nanofillers has occurred and that the



**Fig. 10.** ICP-OES intensity of Si I 251 nm line vs successive number of extractions with 5% HF (by volume) in water for un-irradiated and  $10 \times 10^5$  kJ/m<sup>2</sup> UV-irradiated epoxy/nanosilica composites.

extraction method used in this study did not substantially degrade the crosslinked amine-cured epoxy polymer.

Figure 11(a) displays the average Si mass extracted from blank references and epoxy nanocomposites containing 5% and 10% nanosilica irradiated with  $10 \times 10^5$  kJ/m<sup>2</sup> UV radiation. The relative uncertainties of these results range from 4.6% to 16%, with the lower values associated with 10% nanosilica composites due to greater amounts of SiO<sub>2</sub> nanofillers accumulated on the composite surface. The concentrations of Si extracted from both un-irradiated and irradiated 10% nanosilica composites were substantially higher than those of their corresponding 5% nanosilica samples. This is likely due to the higher nanosilica loading nanocomposite containing greater amounts of SiO<sub>2</sub> nanofillers on both un-irradiated and irradiated surfaces. UV irradiation increased Si amounts in the extracted solutions by factors of 2.3 and 1.7 for the 5% and 10% nanosilica composites, respectively. Further, the observation that some Si were extracted from the un-irradiated specimens is consistent with the presence of SiO<sub>2</sub> nanofillers on the surface of this material, as seen in the AFM images (Fig. 9). Clearly, the extraction did dissolve some SiO<sub>2</sub> particles residing at or near the nanocomposite surface. It should be noted that, because the nanocomposite specimens were completely immersed in the extraction solution, the extracted Si concentrations for both un-irradiated and irradiated specimens were from both the front and back sides of the films. However, the nature (e.g., level of imbedding in the matrix, level of matrix coverage, etc.) of these dissolved nanofillers is unknown. It is speculated that any SiO<sub>2</sub> nanofillers or clusters of SiO<sub>2</sub> nanofillers at or near the surface that were partly or thinly coated with the epoxy matrix were dissolved by the HF extraction solution. In addition, because the surface of this nanosilica material was covered with low surface energy trimethylsilyl groups (Si–O–Si(CH<sub>3</sub>)<sub>3</sub>),<sup>54</sup> its interaction with the epoxy matrix is through weak dispersion forces. Therefore, any SiO<sub>2</sub>

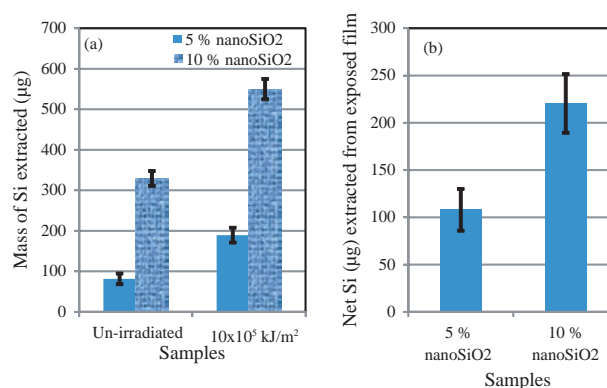


**Fig. 11.** (a) Total masses of Si extracted from un-irradiated and  $10 \times 10^5$  kJ/m<sup>2</sup> UV-irradiated nanocomposites, and (b) Si mass differences between un-irradiated and  $10 \times 10^5$  kJ/m<sup>2</sup> UV-irradiated nanocomposites. All results were the average of eight or nine specimens, and the error bars represent 95% confidence interval.

nanofillers that were not deeply imbedded in the matrix were likely dissolved by the HF extraction.

Because the specimens used for blank references were of the same size and production batch as the irradiated specimens, the extracted Si resulting from the unexposed side and under the surface of the composite can be corrected by subtracting the Si value of the un-irradiated specimen from the Si value of the irradiated specimen. Figure 11(b) illustrates the Si mass difference between the un-irradiated and the UV-irradiated specimens for 5% and 10% nanosilica composites. These Si mass differences correspond to the total amounts of SiO<sub>2</sub> nanofillers on the nanocomposite surface that were generated by the 10 × 10<sup>5</sup> kJ/m<sup>2</sup> UV irradiation, because the contribution of Si from the hexamethyl disilazane surface treatment of the nanosilica was negligible (less than 1% of nanosilica mass as measured by TGA). The results show that the net amount of Si accumulated on the nanocomposite surface after 10 × 10<sup>5</sup> kJ/m<sup>2</sup> UV irradiation for the 10% nanosilica composite was approximately a factor of two greater than that for the 5% nanosilica material irradiated at the same dose (220 μg vs 105 μg).

The amounts of Si extracted by the HF solution can be used to estimate the thickness of the nanosilica layer formed on the nanocomposite surface for each accumulated irradiation dose. For example, the extracted Si masses of 105 μg and 220 μg for the accumulated dose of 10 × 10<sup>5</sup> kJ/m<sup>2</sup> are translated to 225 μg and 471 μg of SiO<sub>2</sub> material accumulating on the 5% and 10% nanosilica composite surfaces, respectively (calculated by using

the molecular mass of 60 g/mol for SiO<sub>2</sub>). Assuming that the SiO<sub>2</sub> nanofillers formed on the nanocomposite surface during UV irradiation were mostly devoid of polymer, compacted tightly, and spread uniformly on the 19 mm diameter specimen surface and by using a density of 2.2 g/cm<sup>3</sup> for silica, the thicknesses of the SiO<sub>2</sub> nanofiller layer formed on the 5% and 10% nanosilica composite surfaces after UV irradiation at 10 × 10<sup>5</sup> kJ/m<sup>2</sup> dose were estimated to be 320 nm and 753 nm, respectively. These values are likely a low estimate, because the SiO<sub>2</sub> layer formed on the nanocomposite surfaces after UV irradiation still contain some organic material, as seen in FTIR (Fig. 6) and XPS (Fig. 7) results. Because the density of a mixture is proportional to its chemical composition and density of a typical polymer is approximately half that of SiO<sub>2</sub> (1.12 g/cm<sup>3</sup> vs 2.2 g/cm<sup>3</sup>), the presence of organic materials in the SiO<sub>2</sub> surface layer will increase its thickness value. An accurate value on the chemical composition of the UV-irradiated surface layer would provide a better thickness estimate. Nevertheless, HF extraction followed by ICP-OES analysis is a good sensitive method to quantify the amount of SiO<sub>2</sub> nanofillers accumulated on the polymer nanocomposite surfaces irradiated with UV radiation. Quantitative data are needed for following the kinetics of nanofillers accumulated on polymer nanocomposites as a result of matrix degradation during exposures to the environments. They are also needed to validate predictive models for the accumulation rate of nanofillers during exposure to photolytic or hydrolytic environments of polymer composites.

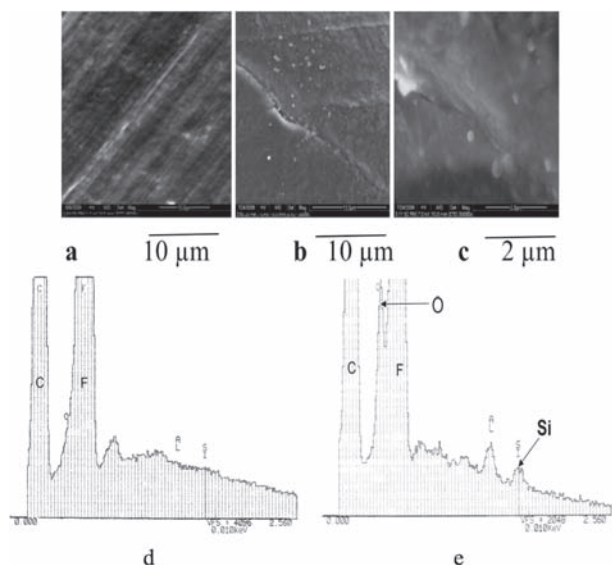


**Fig. 12.** SEM images of the nanofiller collector surface: (a) before, and (b) after UV irradiating an epoxy/5% nanosilica composite specimen with a  $7.0 \times 10^5$  kJ/m<sup>2</sup> dose, (c) higher magnification of b, showing numerous spherical nanoparticles; EDS spectra of nanofiller collector surface; (d) before, and (e) after UV irradiating an epoxy/5% nanosilica composite specimen with a  $7.0 \times 10^5$  kJ/m<sup>2</sup> dose, showing the appearance of Si and O.

### 3.5. Release of SiO<sub>2</sub> Nanoparticles During UV Irradiation

Microscopic and spectroscopic results shown in Figures 5 to 11 strongly suggest that the increase of nanosilica

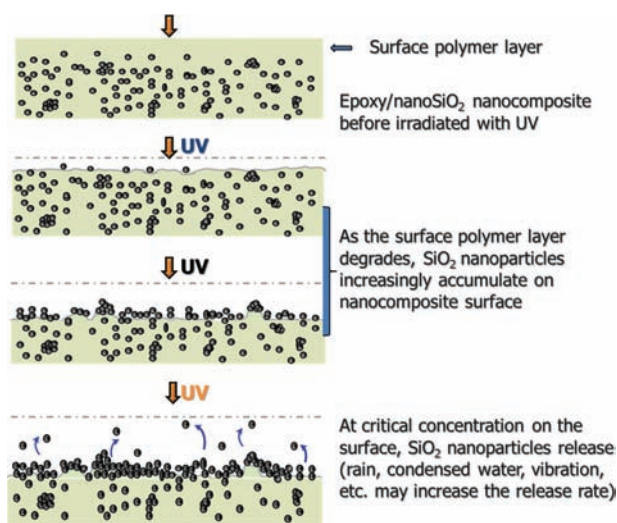


**Fig. 13.** Conceptual model for surface accumulation and release of SiO<sub>2</sub> nanofillers of epoxy/nanosilica composites irradiated with UV radiation.

concentration at the composite surface with UV irradiation was a result of the matrix degradation. However, these results do not fully answer the question: was the SiO<sub>2</sub> nanofiller released from the nanocomposites occur during their UV irradiation? Analysis of particles collected at the bottom of the sample holder addresses this question. Figure 12 shows SEM images and EDS spectra of the particle collector surface before and after a nanocomposite specimen was UV irradiated with a dose of  $7.0 \times 10^5$  kJ/m<sup>2</sup>. Before irradiation, the collector surface showed no evidence of particles (Fig. 12(a)). After  $7.0 \times 10^5$  kJ/m<sup>2</sup> irradiation, many particles were observed on the collector surface (Fig. 12(b)), and numerous spherical nanoparticles can be seen with higher magnification (Fig. 12(c)). The EDS spectrum of the collector surface before the nanocomposite specimen was irradiated showed only fluorine (F) and carbon (C) (Fig. 12(d)), as expected for a poly(tetrafluoroethylene) liner. However, EDS spectrum of the same collector surface after the specimen was irradiated revealed the presence of silicon (Si) element (Fig. 12(e)) and an increased concentration of O. Poly(tetrafluoroethylene) is a highly UV resistant material, and thus the observed concentration increase of O cannot be attributed to the oxidation of this material. The increase of both Si and O implies that the spherical nanoparticles on the collector surface observed in Figure 7(c) were likely the SiO<sub>2</sub> compound. Results of Figure 12 have provided direct evidence that SiO<sub>2</sub> nanofillers or their aggregated form were released from the epoxy nanocomposites to the surroundings during their UV irradiation with 295 nm–400 nm radiation. However, these preliminary results do not establish whether these released SiO<sub>2</sub> nanofillers are pristine or coated with polymer. Such information is important for assessing the potential risks of released nanofillers, because nanomaterials that are covered with an inert polymer layer are less likely to impart an EHS concern than the pristine nanomaterials do. Work is in progress to address this question.

Based on microscopic and spectroscopic evidence, SiO<sub>2</sub> nanofiller release during UV irradiation of amine-cured epoxy nanocomposites used in this study likely followed the sequence shown in Figure 13. First, the epoxy matrix layer on and near the nanocomposite surface underwent photodegradation and was removed. This resulted in a gradual increase of the number of SiO<sub>2</sub> nanofillers on the specimen surface with irradiation dose. At a critical thickness/concentration, particles containing SiO<sub>2</sub> fell off the vertical surface (release), likely due to gravitation force. For nanocomposites exposed to outdoor, environmental elements such as rain, condensed water, wind, mechanical vibration, and stresses resulting from materials dimensional changes likely affect the nanofiller release rate. Since most common polymers are susceptible to degradation during exposures to the UV environment,

even with those containing UV stabilizers, this conceptual model for the release of SiO<sub>2</sub> nanofillers should be applicable to other polymers and to other low aspect ratio, spherical nanofillers used in polymer nanocomposites and nanocoatings.

#### 4. CONCLUSIONS

Nanofillers are increasingly used to enhance performance properties of polymeric materials in many high volume exterior applications. Because polymers are susceptible to photodegradation by solar UV radiation, nanofillers in a polymer nanocomposite can be released into the environments during their life cycle. Such release raises possible environment, health and safety effects that may hinder the commercialization of these advanced materials. This study has investigated the fate and release of SiO<sub>2</sub> nanofillers from epoxy/nanosilica composites irradiated with 295 nm to 400 nm UV radiation. Based on experimental results of chemical degradation, mass loss, surface morphology, surface accumulation, and nanofiller release, the following conclusions can be made:

- (1) Amine-cured epoxy matrix in the nanocomposite underwent photodegradation during irradiation with 295 nm to 400 nm UV light, resulting in substantial mass loss and an increase in nanofiller concentration on irradiated nanocomposite surfaces.
- (2) The rate of mass loss of epoxy/nanosilica composites was greater than that of the neat epoxy, but the rate of matrix degradation appeared similar between epoxy/nanosilica composites and neat epoxy.
- (3) A method based on HF extraction followed by ICP-OES analysis has been developed to quantify the amount of nanosilica accumulation on the composite surface irradiated with UV radiation.
- (4) Microscopic and spectroscopic analyses showed conclusively that SiO<sub>2</sub> nanofillers were released to the environment after a relatively low UV irradiation dose.
- (5) A conceptual model for the accumulation and release of SiO<sub>2</sub> nanofillers during UV irradiation has been proposed, which should be applicable to other polymers and other types of spherical nanofillers.

The results of this study provide helpful information to assess the potential risk of nanosilica accumulation and release during life cycles of a polymer nanocomposite. Work is under way to predict the SiO<sub>2</sub> nanofiller release rate and to characterize chemical composition of the released particles.

**Acknowledgments:** The authors would like to acknowledge the Materials Science Department at Johns Hopkins University for use of the surface analysis laboratory.

## References and Notes

1. T. McNally and P. Pötschke (Eds.), *Polymer-Carbon Nanotube Composites, Preparation, Properties, and Applications*, Woodhead Publishing, Philadelphia (2011).
2. P. C. Ma, N. A. Siddiqui, G. Marom, and J. K. Kim, *Composites Part A – Appl. Sci. Manufact.* 41, 1345 (2010).
3. P. M. Ajayan and J. M. Tour, *Nature* 447, 1066 (2007).
4. J. R. Potts, D. R. Dreyer, C. W. Bielawski, and R. S. Ruoff, *Polym.* 52, 5 (2011).
5. H. Kim, A. Abdala, and C. Macosko, *Macromol.* 43, 6515 (2010).
6. B. Li and W. H. Zhong, *J. Mat. Sci.* 46, 5595 (2011).
7. S. Pavlidou and C. D. Papaspyrides, *Prog. Polym. Sci.* 33, 1119 (2008).
8. B. Chen, J. R. G. Evans, H. C. Greenwell, P. Boulet, P. V. Coveney, A. A. Bowden, and A. Whiting, *Chem. Soc. Rev.* 37, 568 (2008).
9. H. Zou, S. S. Wu, and J. Shen, *Chem. Rev.* 108, 3893 (2008).
10. D. R. Paul and L. M. Robeson, *Polym.* 49, 3187 (2008).
11. A. Helland, P. Wick, A. Koehler, K. Schmid, and C. Som, *Env. Health Persp.* 115, 1125 (2007).
12. A. Nel, T. Xia, L. Mädler, and N. Li, *Sci.* 311, 622 (2006).
13. C. Poland, R. Duffin, I. Kinloch, A. Maynard, W. A. H. Wallace, A. Seaton, V. Stone, S. Brown, W. MacNee, and K. Donaldson, *Nat. Nanotechnol.* 3, 423 (2008).
14. A. D. Maynard, *Nanotoday* 2, 22 (2006).
15. C. W. Lam, J. T. James, R. McCluskey, S. Arepalli, and A. Hunter, *Crit. Rev. Toxicol.* 36, 189 (2006).
16. K. Aschberger, H. Johnson, V. Stone, R. Aitken, S. Hankin, S. Peters, C. Tran, and F. Christensen, *Crit. Rev. Toxicol.* 40, 759 (2010).
17. R. D. Handy, T. B. Henry, T. M. Scown, B. D. Johnston, and C. R. Tyler, *Ecotoxicol.* 17, 396 (2008).
18. L. K. Adams, D. Y. Lyon, and P. J. J. Alvarez, *Water. Res.* 40, 3527 (2006).
19. E. J. Petersen, B. C. Nelson, *Anal. Bioanal. Chem.* 398, 613 (2010).
20. E. J. Petersen, R. A. Pinto, D. J. Mai, P. F. Landrum, W. J. Weber, *Environ. Sci. Technol.* 45, 1133 (2011).
21. J. Lee, S. Mahendra, and P. J. J. Alvarez, *ACS Nano* 4, 3580 (2010).
22. Gottschalk and B. Nowack, *Environ. Monit.* 13, 1145 (2011).
23. D. Gohler, M. Stintz, L. Hillemann, and M. Vorbau, *Ann. Occup. Hyg.* 54, 615 (2010).
24. M. Vorbau, L. Hillemann, and M. Stintz, *J. Aerosol Sci.* 40, 209 (2009).
25. L. Golanski, A. Gaborieau, A. Guiot1, G. Uzu, J. Chatenet, and F. Tardif, *J. Phys.: Conf. Ser.* 304, 012062 (2011).
26. D. Bello, B. Wardle, N. Yamamoto, R. deVilloria, E. Garcia, A. Hart, K. Ahn, M. Ellenbecker, and M. Hallock, *J. Nanoparticle Res.* 11, 231 (2009).
27. W. Wohlleben, S. Brill, M. W. Meier, M. Mertler, G. Cox, S. Hirth, B. vonVacano, V. Strauss, S. Treumann, K. Wiench, L. Ma-Hock, and R. Landsiedel, *Small.* (2011), DOI: 10.1002/sml.201002054.
28. E. J. Petersen, L. Zhang, N. T. Mattison, D. M. O'Carroll, A. J. Whelton, N. Uddin, T. Nguyen, Q. Huang, T. B. Henry, R. D. Holbrook, and K. Chen, *Env. Sc. Technol.* in Press (2011).
29. R. Kumar and H. Münnstedt, *Biomater.* 26, 2081 (2005).
30. T. Benn and P. Westerhoff, *Env. Sci. Technol.* 42, 4133 (2008).
31. T. Benn, B. Cavanagh, K. Hristovski, J. D. Posner, and P. Westerhoff, *J. Env. Qual.* 39, 1 (2010).
32. L. Geranio, M. Heuberger, and B. Nowack, *Env. Sci. Technol.* 43, 8113 (2009).
33. I. Armentano, M. Dottori, D. Puglia, and J. M. Kenny, *J. Mater. Sci.: Mater. Med.* 19, 2377 (2008).
34. M. van der Zande, B. Sitharaman, X. F. Walboomers, L. Tran, J. S. Ananta, A. Veltien, L. J. Wilson, J. I. Alava, A. Heerschap, A. G. Mikos, and J. A. Jansen, *Tiss. Eng. C* 17, 19 (2011).
35. L. Hsu and H. Chein, *J. Nanopart. Res.* 9, 157 (2007).
36. A. Iacomino, G. Cantele, D. Ninno, I. Marri, and S. Ossicini, *Phys. Rev. B* 78, 075405 (2008).
37. R. Kaegi, A. Ulrich, B. Sinnet, R. Vonbank, A. Wichser, S. Zuleeg, H. Simmler, S. Brunner, H. Vonmont, M. Burkhardt, and M. Boller, *Environ. Pollut.* 156, 233 (2008).
38. M. Kamal and B. Huang, *Handbook of Polymer Degradation*, Edited by S. Hamid, M. Amin, A. Maadhah, Marcel Dekker, New York (1992), p. 127.
39. T. Nguyen, W. E. Byrd, D. Alshed, J. W. Chin, C. Clerici, J. W. Martin, *J. Adhesion* 83, 587 (2007).
40. X. Gu, G. Chen, M. Zhao, S. Watson, T. Nguyen, J. W. Chin, and J. W. Martin, *J. Coat. Technol. Res.* In Press (2011).
41. C. Hegedus, F. Pepe, D. Lindenmuth, and D. Burgard, *J. Coat. Technol. Tech. April*, 42 (2008).
42. R. Li and H. Zhao, *Polym.* 47, 3207 (2006).
43. National Nanotechnology Initiative, *Env., Health, and Safety, Res. Strat.* (2011).
44. T. Nguyen, B. Pelligrin, C. Bernard, X. Gu, J. M. Gorham, P. Stutzman, D. Stanley, A. Shapiro, E. Byrd, J. Hettenhouser, and J. W. Chin, *J. Phys. Conf. Ser.* 304, 012060 (2011).
45. T. Nguyen, B. Pelligrin, L. Mermet, A. Shapiro, X. Gu, and J. W. Chin, *Proc. Nanotechnol.* (2009).
46. C. Bernard, T. Nguyen, B. Pelligrin, R. D. Holbrook, M. Zhao, and J. W. Chin, *J. Phys. Conf. Ser.* 304, 012063 (2011).
47. M. Sangermano, G. Malucelli, E. Amerio, A. Priola, E. Billi, and G. Rizza, *Prog. Org. Coat.* 54, 134 (2005).
48. T. I. Yang, R. N. C. Brown, L. Kempel, and P. Kofinas, *Nanotechnol.* 22, 105601 (2011).
49. C. Sow, B. Riedl, P. Blanchet, *J. Coat. Technol. Res.* 8, 211 (2011).
50. H. Zhang, L. Tang, L. Zhou, C. Eger, and Z. Zhang, *Comp. Sci. Technol.* 71, 471 (2011).
51. J. Y. Seo and M. Han, *Nanotechnol.* 22, 025601 (2011).
52. K. O. Yu, C. M. Grabinski, A. M. Schrand, R. C. Murdock, W. Wang, B. H. Gu, J. J. Schlager, and S. M. Hussain, *J. Nanopart. Res.* 11, 15 (2009).
53. X. Lu, Y. Tian, Q. Zhao, T. Jin, S. Xiao, and X. Fan, *Nanotechnol.* 22, 055101 (2011).
54. P. Ariano, P. Zamburlin, A. Gilardino, R. Mortera, B. Onida, M. Tomatis, M. Ghiazza, B. Fubini, and D. Lovisolo, *Small* 7, 766 (2011).
55. K. O. Yu, C. M. Grabinski, A. M. Schrand, R. C. Murdock, W. Wang, B. Gu, J. J. Schlager, S. M. Hussain, *J. Nanopart. Res.* 11, 15 (2009).
56. C. M. Sayes, K. L. Reed, S. Subramoney, L. Abrams, and D. B. Warheit, *J. Nanopart. Res.* 11, 421 (2009).
57. J. Mathias and G. Wannemacher, *J. Coll. Int. Sci.* 125, 61 (1988).
58. J. W. Chin, E. Byrd, N. Embree, J. Garver, B. Dickens, N. T. Fin, and J. W. Martin, *Rev. Sci. Inst.* 75, 4951 (2004).
59. S. A. Rabb, L. Yu, C. Bernard, and T. Nguyen, *Proc. Nanotechnol.* (2010).
60. J. F. Rabek, *Polymer Photodegradation: Mechanism and Experimental Methods*, Chapman and Hall, NY (1995), pp. 185–216.
61. V. Bellenger, C. Bouchard, P. Claveirole, and J. Verdu, *Polym. Photochem.* 1, 69 (1981).
62. V. Bellenger and J. Verdu, *J. Appl. Polym. Sci.* 30, 363 (1985).
63. N. Grassie, M. I. Guy, and N. H. Tennent, *Polym. Deg. Stab.* 14, 209 (1986).
64. A. Rivaton, L. Moreau, and J.-L. Gardette, *Polym. Deg. Stab.* 58, 333 (1997).
65. B. Mailhot, S. Morlat-Therias, M. Ouahioune, and J.-L. Gardette, *Macromol. Chem. Phys.* 206, 575 (2005).
66. A. Rezig, T. Nguyen, D. Martin, L. Sung, X. Gu, J. Jasmin, and J. W. Martin, *J. Coat. Technol. Res.* 1, 173 (2006).
67. X. Gu, D. Stanley, E. Byrd, B. Dickens, W. Meeker, T. Nguyen, and J. W. Martin, *Service Life Prediction of Polymeric Materials*,

- Edited by J. W. Martin, R. A. Ryntz, J. W. Chin, and R. A. Dickie, Springer, NY (2009), p. 1.
68. T. Nguyen, J. W. Martin, E. Byrd, and N. Embree, *J. Coat. Technol.* 75, 37 (2003).
69. D. Raghavan, X. Gu, M. Van Landingham, and T. Nguyen, *J. Polym. Sci., Polym. Phys.* 39, 1460 (2001).
70. X. Gu, T. Nguyen, D. Ho, M. Oudina, D. Martin, B. Kidah, J. Jasmin, A. Rezig, L. Sung, J. C. Jean, and J. W. Martin, *J. Coat. Technol. Res.* 2, 547 (2005).
71. I. Armentano, M. Dottori, D. Puglia, and J. M. Kenny, *J. Mater. Sci. Mater. Med.* 19, 2377 (2008).
72. L. Chen, T. Nguyen, X. Gu, M. Fasolka, and J. W. Martin, *Langmuir* 25, 3494 (2009).

Received: 23 December 2011. Accepted: 13 April 2012.